ALGORITHMIC SYSTEM FOR IDENTIFYING BIRD RADIO-ECHO AND PLOTTING RADAR ORNITHOLOGICAL CHARTS

Leonid Dinevich and Yossi Leshem

ABSTRACT

Dinevich L., Leshem Y. 2007. *Algorithmic system for identifying bird radio-echo and plotting radar ornithological charts.* Ring 29, 1-2: 3-40.

The territory of Israel is a route for major bird migration from Europe and certain areas in Asia and Africa and back. During the period of intensive migration, the average density of birds may reach over 500 birds per a square kilometre of the air. These figures, alongside with the fact the air over the country is saturated with aircraft, makes it an urgent task to find solutions for prevention of disasters caused by aircraft-bird collisions.

In the present paper, a new algorithm is proposed aimed at identifying bird radar echoes against the background of other reflectors. The implementation of the algorithm has made it possible to improve the computerised radar system for bird monitoring developed earlier in Israel on the basis of MRL-5 meteorological radar station. The time needed for echo selection has been significantly reduced, while the trustworthiness of the ornithological data provided by the algorithm has increased. The new algorithm utilizes several echo properties that have been added to the algorithm previously developed by the authors, the most important of them being the pattern of echo movement. These properties in combination with a set of techniques used for their identification enabled to isolate the echo from moving birds against the background of other objects (ground clutter, clouds, atmospheric inhomogeneities, aircraft, *etc.*) at the accuracy level sufficient for operational purposes. The information on echo movement was used for plotting flight vectors (velocity and direction) of individual birds and bird groups. On the basis of movement pattern, four types of movement were distinguished: straightforward at non-uniform velocity; straightforward at uniform velocity; significant deviation from a straight line, non-uniform velocity and chaotic undirected shifts. The system enables on-line plotting of operational ornithological charts every 15-30 min, including charts that combine meteorological and bird monitoring data, to be provided to air traffic control services. This makes the proposed radar ornithological system an efficient means of maintaining air traffic safety in complicated meteorological and ornithological conditions.

L. Dinevich, Y. Leshem, George S. Wise Faculty of Natural Sciences, Dept. of Zoology, Tel-Aviv University, Ramat Aviv, 69978, Israel, E-mail: dinevich@barak-online.net

---

Key words: radar ornithology, radar meteorology, radio-echo, birds, bird migration, ornithology, air traffic safety.

INTRODUCTION

Major routes of bird migration from Europe and, in part, from Asia and Africa and back lie over the territory of Israel (Leshem and Yom-Tov 1998). According to studies, during migration period here the average number of birds per square kilometer of air can exceed 500 (Bruderer 1992). Alongside with the fact that the airspace is crowded with various aircraft, massive intercontinental bird migration in spring and autumn causes aviation accidents (Bahat and Ovadia 2005). Accidents caused by aircraft collisions with birds are a known phenomenon in other world regions (Thorpe 2005, Richardson and West 2005).

These facts have motivated researchers to look for ways of increasing air traffic safety during mass bird migration. Eastwood (1967) noted in his review the potential of various pulse devices as means for bird detection. Numerous studies (Atlas 1964, Houghton 1964, Ganja *et al.* 1991, Bruderer and Liechti 1995, Bruderer 1997, Gauthreaux *et al.* 1998, Zrnic and Ryzhkov 1998, Buurma 1999, Gauthreaux and Belser 2003 and other) describe specific echo properties that enable to identify echo from birds against the background of other reflecting objects, as well as assess the efficiency of using different wave lengths and radar types for ornithological purposes.

On the basis of these studies, the authors of the present paper developed a radar ornithological station aimed at supplying air traffic control with complete data on bird movement. The most important elements of the task were providing the data in real-time mode, covering large areas of air flights and providing data on main flight characteristics, such as height, velocity, direction and density, regardless the time of the day and weather conditions. Providing these data to air traffic control, especially in case of jet flights, may help reduce the number of aircraft-bird collisions. To solve this task, a research was needed in order to find new characteristics of bird echo. In Israel, the data, as in the previous study, was obtained by means of MRL-5 radar.

MRL-5, which is a high-grade meteorological radar designed mainly for cloud monitoring, has a capability of full azimuth scanning (0-360), the elevation range of -2 to +90 in the upper hemisphere and a symmetric narrow beam operating simultaneously at two wave lengths (3 cm and 10 cm).

The main parameters of MRL-5 station are presented in Table 1.

Simultaneous operating of the two wave lengths provides the equality of radar scopes and potentials of both transceivers. Thus, one can consider the ratio of radar echo on the two wave lengths to be a function of the target properties entirely. A detailed description of the station can be found in Abshayev *et al.* (1980).

The research previously conducted with the help of MRL-5 enabled the authors to develop a method and an algorithm for selecting bird echoes (Dinevich *et al.* 2000, Dinevich *et al.* 2004). Implementation of the algorithm revealed a number of drawbacks, which alongside with the newly found properties made it possible to develop

a new algorithm for bird echo detection. The advantages of the new algorithm are higher reliability and computation rate.

Table 1
Principal performance characteristics of the MRL-5 Radar

Parameter	Symbol	Measurement	Channels	
		Unit	1	2
Wave length	λ	cm	3.14	10.15
Peak pulse	Pt	kW	250	800
Pulse length	τ	$\mu\sigma$	1; 2	1; 2
Repetition frequency	F	Hz	500; 250	500; 250
Diameter of antenna paraboloid		m	1.4*; 4.5**	4.5
Beam width		deg	0.5; 1.5	1.5
Azimuth angle rate	$n1$	rotations/min	0...6	0...6
Elevation angle rate	$n2$	scans/min	0...6	0...6
Receiver sensitivity	PO	dB/W	130	140

* beamwidth of 0.5 is formed on the first channel while using antenna of 1.4 m in diameter
** beamwidth of 1.5 is formed on the first channel while using antenna of 4.5 m in diameter

The new algorithm and technique developed for its implementation in real-time mode has been used for two years by Israeli air control services in order to provide aviation safety in periods of spring and autumn bird migration.

FORMULATION OF THE TASK

The new algorithm is based on the previously developed radar system (Dinevich *et al.* 2004), which makes it necessary to describe only the major features of the task.

1. Collecting data on all the radar echo within the upper hemisphere, within the radius of 60 km (the centre being the radar location). Data collection was performed in two automatic antenna modes:
   a) Mode for collection and selection of echo for the purposes of bird detection. Circular antenna scans are performed, with tilt angle ranging between 0 to n , where n can vary depending on the actual bird flight height. Usually, n is 6-12 . Antenna elevation is performed automatically at a preset interval, which is usually equal to the double value of antenna beam. At every preset tilt angle, several scans are run (normally 7-10 scans). Antenna rotation rate is one revolution per 10 s.
   b) Mode for collection and selection of echo for cloud and precipitation monitoring. Circular antenna scans are performed, with tilt angle ranging between 0 and 85 . Antenna elevation is performed automatically at a preset interval. At each tilt angle, antenna runs only one scan. Antenna rotation rate is one revolution per 10 s.
2. Digitally-processed signals are entered into computer and undergo filtration. In order to amplify the “signal/noise” dependence, signals are summed up over

several monitoring pulses (usually 16 pulses). Signal calibration is performed systematically, using the calculated values of the radar constant and measurements of the receiver noise. On the basis of the calibration curve obtained for both receivers, useful signals undergo digital transformation and are sent for further processing in case their power does not exceed the noise level by more than 4-5 dB (*i.e.* remains within the range suitable for identifying useful signals). Bird echo power (Z) is measured in dB or dBZ in relation to the noise level (the station sensitivity). The power of echo from clouds and ground clutter is measured in lg$Z$.

3. In order to increase the efficiency of the station, data collection was performed more frequently that it is actually needed for the given level of radar resolution. Distance quantization (60 km) is 1024, azimuth quantization is 2048. The resolution parameters of the radar and the registration system are presented in Table 2. In the coordinates of "distance-angle", each bird is presented not as a dot but as a "spot".

Table 2
Resolutions parameters of the radar and the registration system

	Radar	Registration
Azimuth resolution	0.5 ; 1.5	0.176
Distance resolution	150 m	60 m

4. Selection and analysis of echo from clouds and precipitation are performed on the basis of the algorithm developed in Abshayev *et al.* (1984).
5. The algorithm for bird echo selection comprises three main stages:
   a) Analysis of signals' power and their selection by the power level. On the lower level, there are signals with the weakest power (in relation to the noise level) that the computer was able to pick up. On the upper level, there are signals whose power exceeds the values that can be reflected by bird echoes (usually $Z > 30$ dBZ).
   b) Contouring the area occupied by a signal from a flying bird (group of birds), and isolation of each bird (group of birds) from other reflecting objects. The idea underlying this stage is the following. A signal reflected from a flying bird changes its location on successive scans because the bird is moving. Upon summation of the scans, coordinates of the signal centres form an almost straight line. The technique of contouring the summated echo, provided the echo is uninterrupted, enables to obtain an area elongated in the direction of the movement. The area, formed as the result of accumulating data from scan to scan, can be represented as an ellipse. The larger axis of the ellipse can be approximated by a vector whose length characterizes the velocity, while its orientation towards the cardinals characterizes the direction of a bird's flight. Signals from static objects or those chaotically oriented towards the direction of movement are unable to form the said ellipse and, therefore, cannot be bird echoes.

c) Calculating the velocity vector for each bird (bird group) and selecting by the criterion of correlation coefficient.

6. The program ensures that, out of 7-9 echoes available, not fewer than 5 successive echoes are situated within an area approximating to a straight line.

Assessment of the data obtained by the described algorithm for bird echo selection revealed a problem that significantly affects the outcome of the procedure. Essentially, the problem is as follows. Powers of radar echoes from smaller birds or birds flying far from the radar drop beneath the noise level due to their fluctuation in time over a series of scans (Houghton 1964, Eastwood 1967, Bruderer and Joss 1969).

This can be accounted for by several reasons, among them alterations in the power of bird echo due to a change in the position of its wings. For instance, the echo obtained within the first scan may be reflected from a bird with its wings spread. The echo was above the noise level and registered in the echo field of the given scan. During the second scan (10 s later), the echo was reflected from the same bird while its wings were folded. The power of this echo may be beneath the noise level and will not fall within the echo field of the second scan. The frequency of such fluctuations may reach 2-50 Hz (Chernikov 1979).

Similar effects can occur when the position of a bird changes in relation to its orientation towards the radar. It can be clearly seen in Table 3 presenting the measured values of the effective scattering area (ESA – σ) in m^2 for some bird species with their wings folded (Edwards and Houghton 1959). In the study that measured σ of birds at various angles in relation to the pulse beam in an anechoic chamber (Zavirucha *et al.* 1977), the echo maximum was found to be within the range of 65 to 115 in relation to the beam direction, which corresponds to bird's lateral surface. Due to these reasons, the value may either increase by ten-fold of the mean value or drop almost to zero.

Table 3
ESA (σ) values for various bird species with wings folded, their bodies set at different angles in relation to the radar

Bird species	Dimensions of bird σ (m^2) obtained at exposure at various angles		
	Side	Head	Tail
Rook	$2.5 \quad 10^{-2}$	–	–
Pigeon	$1.0 \quad 10^{-2}$	$1.1 \quad 10^{-4}$	$1.0 \quad 10^{-4}$
Starling	$2.5 \quad 10^{-3}$	$1.8 \quad 10^{-4}$	$1.3 \quad 10^{-4}$
House Sparrow	$7.0 \quad 10^{-4}$	$2.5 \quad 10^{-5}$	$1.8 \quad 10^{-5}$

These factors prevent the algorithm from meeting the basic requirement of obtaining not fewer that 5 echo points arranges in succession, out of the series of 7-9 scans. Due to the above mentioned reasons, the expected echo movement track is interrupted and cannot be detected by the contouring technique stipulated for the

method. Instead of an elongated ellipse, the summated echo forms several spots that have complex shapes and are separated from one another. The procedure excludes such signals from the analysis.

The interruption of the expected lines occurs also in case when:

a) the velocity of a bird flight exceeds the velocity that enables echo "spots" to form an uninterrupted sequence. At such velocities, the echo spots are distant from one another, do not form a continuous area and thus cannot be contoured.
b) the radar observes birds that repeatedly alter the vertical profile of flight. For instance, certain smaller birds make pauses between wing flappings. During the pause, they fold their wings completely, retaining the high speed but losing the height. With the next wing flapping, they gain the height back, *etc*. In case of such flight pattern, the bird echo may periodically appear in successive scans on the level of the radar beam width, or go beyond it.

All this means that the contouring technique, implemented in the above-described algorithm for identifying bird echo, in some cases is not reliable enough and has to be replaced by another procedure.

THE MAIN IDEA UNDERLYING THE NEW ALGORITHM

Table 4 shows characteristics typical of echo from migrating birds, accumulated throughout long-term observations. In course of the present study, additional echo characteristics have been found.

Figure 1 (A, B) shows bird echo fields obtained by way of photographing the radar screen during horizontal scanning at a constant vertical angle, using the following two modes:

a) the camera shuttle was kept open during a single scan, duration – 10 s, vertical angle – 3
b) the camera shuttle was kept open during 18 scans, duration – 3 min, tilt angle – 3

Figure 2 shows the same echo field after the digital data processing and data summation over 18 scans.

Comparative analysis of the three pictures shows that the main common characteristic of bird echo is its specific movement, resulting in transformation of dotty radio-echo (Fig. 1A) into streaks (Fig. 1B). The streaks are relatively straightforward (Fig. 1B, Fig. 2). The increments in the length of the streaks take place as the result of the echoes' forward movement from scan to scan. At the same time, the number of echo dots forming most streaks is smaller than the number of scans, hence the straightforwardness of streaks is disrupted by a change of direction. To sum up, bird echoes do move, and this movement has several pronounced distinguishing characteristics.

Table 4
Typical characteristics of echo from migrating birds

Typical characteristics of radar echo	Studies*
• Relatively low power. Reflectance coefficient – $Z < 30$ dBZ. • Forward and relatively linear movement. • Maximum amplitude fluctuations within the low frequency range (below 10 dB in 2-50 Hz frequency range). • MRL-measured σ^{**} are greater on the 10 cm wave length than those on the 3 cm wave length. • Polarization characteristics of the signal are typical of horizontally--oriented targets. Differential reflectance as the ratio of horizontally-oriented signal (with pulse horizontally polarized) to vertically-oriented signal (with pulse vertically polarized) exceeds the unity significantly ($dP = P_{\text{È}} / P\text{Ç} >> 1$). For small droplets within clouds and precipitation this value is close to unity. • In the wave length range of λ from 3 cm to 100 cm, σ of birds and insects decrease noticeably as the radar wave length increases. At the same time, there is a distinct maximum of the σ (λ) frequency dependency that occurs at λ =10 cm wave length. • High dispersion of experimental data at $\lambda = const.$ (from few tens of cm^2 at λ = 3 cm to $\sigma = 10^{-1}$ cm^2 at λ = 100 cm). • The mean σ-values of different bird spiecis at the value of radar wave length less than 10 cm from 15 cm^2 (Sparrow) up to 400 cm^2 (Albatross). • σ-values of birds are approximately by order of 2-3 greater than σ-values of insects.	Houghton 1964, Chernikov and Shupjatsky 1967, Eastwood 1967, Hardy and Katz 1969, Bruderer and Joss 1969, Kropfli 1970, Skolnik 1970, Zavirucha *et al.* 1977, Chernikov 1979, Ganja *et al.* 1991, Bruderer 1992, Gauthreaux *et al.* 1998, Miller *et al*. 1998, Russell and Gauthreaux 1998, Buurma 1999, Venema and Russchenberg 2000, Gudmundsson *et al.* 2002, Komenda-Zehnder *et al.* 2002, Larkin *et al.* 2002, Gauthreaux and Belser 2003.

* table presents only a small part of the numerous studies of bird echo characteristics
** ESA (σ) – scattering cross-section

We photographed the radar screen, the primary task being to find a simple way of selecting signals from birds on the photos. For this purpose, the camera shuttle was kept open during 1.5 min for each picture, with the help of a special valve and a timer. During this time interval, the radar beam, at the antenna scan rate of 6 revolutions per minute, performed 9 revolutions. The dotted signals from birds were converted into lines, forming a certain pattern of tracks, the length of such tracks corresponding to birds' flight velocities. The direction of bird flights was easily determined by the shift of dotted echo on the screen. Aiming the radar beam strictly to the north or to the south and registering the radio-echo shifts within a preset time interval (1.5 min), we obtained both the velocity and the direction of bird flights.

It was found that flight directions have a predominantly southern component in autumn and a northern component in spring. In rare cases, usually in those of non-migratory flights, these tracks have chaotic spatial orientation. Dotted echoes or area echoes that do not change their spatial position with time are not related to birds. Reflections from aircraft, due to their high velocities, are converted into dotted lines on the photos and could be easily identified. Figures 1 (A, B) and 2 shows dotted echo from birds, as well as tracks of both distinctly directed and chaotic movements of birds' echoes.

A

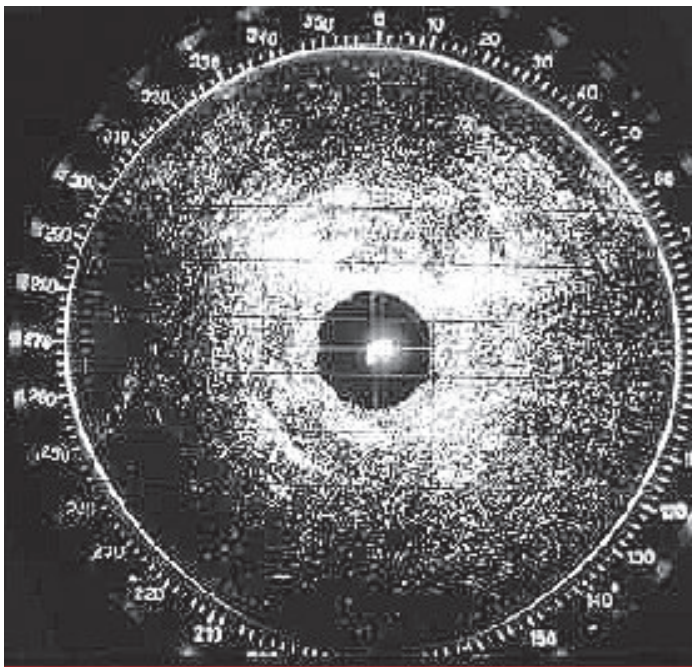

B

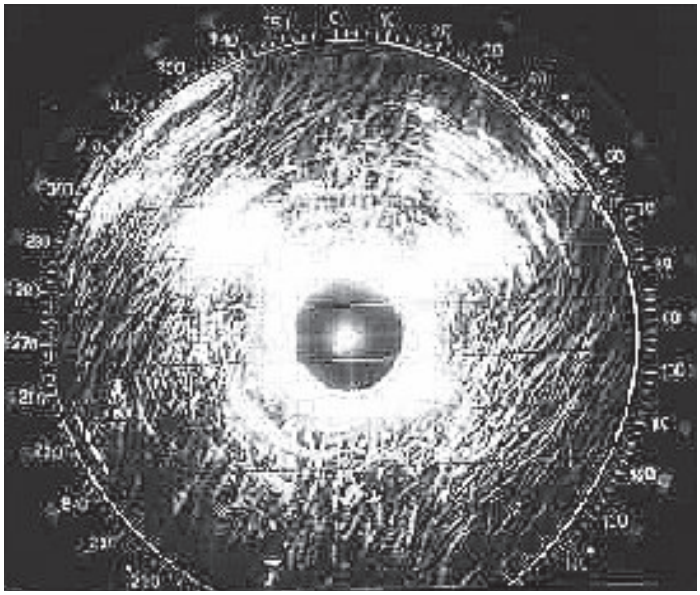

Fig. 1. Photos of circular scan screen. Echoes are received within the range of the radar sensitivity.
A. Single scan performed at night-time. Exposure duration – 10 s. Tilt angle – 3 . Dot echoes are reflected from birds.
B. The same as in A, but over 18 scans together. Exposure duration – 3 min. Tilt angle – 3 . Dot echo seen in A have been transformed into tracks (bird flight trajectories). Lines formed by dotted echo represent bird flight tracks, other lines are echoes from hills.

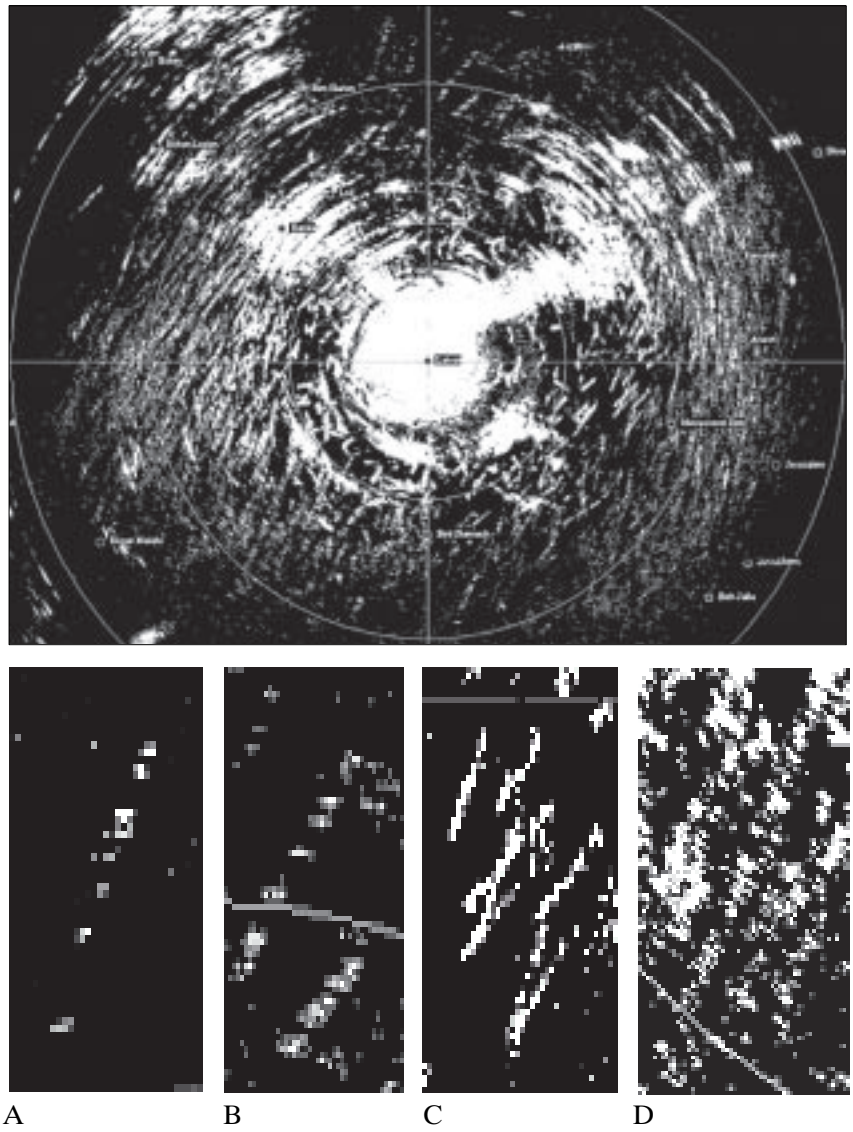

Fig. 2. The echo field is identical to that in Fig. 1B, presenting the data after digital processing prior to bird echo selection. Lines formed by successive dotted echo are bird flight trajectories. Areal shapeless echo are reflections from hills. In the fragments isolated one can clearly see how bird flight trajectories are formed by dotted echo, such as: A – a single bird or bird group; B – two birds or two bird groups; C – several birds or bird groups; D – many birds or bird groups in zones of high bird density.

The following data were obtained as a result of 200 experimental observations over bird echo movements both on the radar screen and the oscillograph (made both in the daytime and at night). In a series of 8 scans (80 s) at a fixed tilt angle

within a 60 km radius, the radar registered moving bird echoes at a preset coordinate (a spot within the scan area with coordinates *X*, *Y*, *Z* and dimensions determined by the radar resolution parameters). In 68% of cases, moving echoes were registered once, in 27% of cases twice, and in 5% of cases three times.

A specially designed program enabled to analyse the structure of over 150 randomly selected echo streaks. All the streaks were obtained as a result of summing-up data over 8 scans. The angle was chosen with the goal of excluding as much ground clutter echo as possible. The program enables to trace the formation of echo streaks from scan to scan. The results obtained show that in about 90% of cases, the echoes occurred twice at the same point during the 80 s long series of eight scans. This result can be accounted for by both the character of birds' movements and the technical parameters of the radar system, with its short impulses and the narrow symmetric beam (Table 2). In contrast, the echoes from ground clutter, clouds and some atmospheric heterogeneities were usually registered as recurring.

The only exception is weak signals with pronounced fluctuation reflected from porous clouds and precipitation. In case such "blinking" signals are relatively dense within a limited area (of about 2-10 km^2 in square and up to 2 km in height), they create an illusion of spatial movement. In some cases, such signals were registered as recurring at the same point twice during the eight scans, which is similar to the recurrence of bird echoes. However, subsequent echoes of these targets are not located along a direct line, but are rather scatted chaotically, thus forming chaotically directed vectors as opposed to those formed by echoes of migrating birds. This characteristic is the basis for detecting the areas of these problematic echoes and is hereafter referred to as the state-of-chaos coefficient.

To sum up, when we exclude all the echo that recur more than twice at the same point from the overall 8-scan data, we will exclude ground clutter echo and "lose" echo of not more than 5-10% of birds. The remaining echoes are to be analysed against a set of properties described above, first and foremost by the pattern of movement.

The principle underlying the system remains unchanged (Dinevich *et al.* 2004), while selection of bird echo is performed on the basis of the abovementioned properties and considerations.

THE SCHEME OF THE ALGORITHM

Figure 3 shows the flowchart of the new algorithm developed in the present study for identifying birds and estimating their flight velocities. To sum up, the main stages of the algorithmic processing of radio-echo fields, described in detail in the preceding sections of the paper, are as follows:

1. Summating the totality of radio-echo (those above the noise level) over a prescribed number of scans.

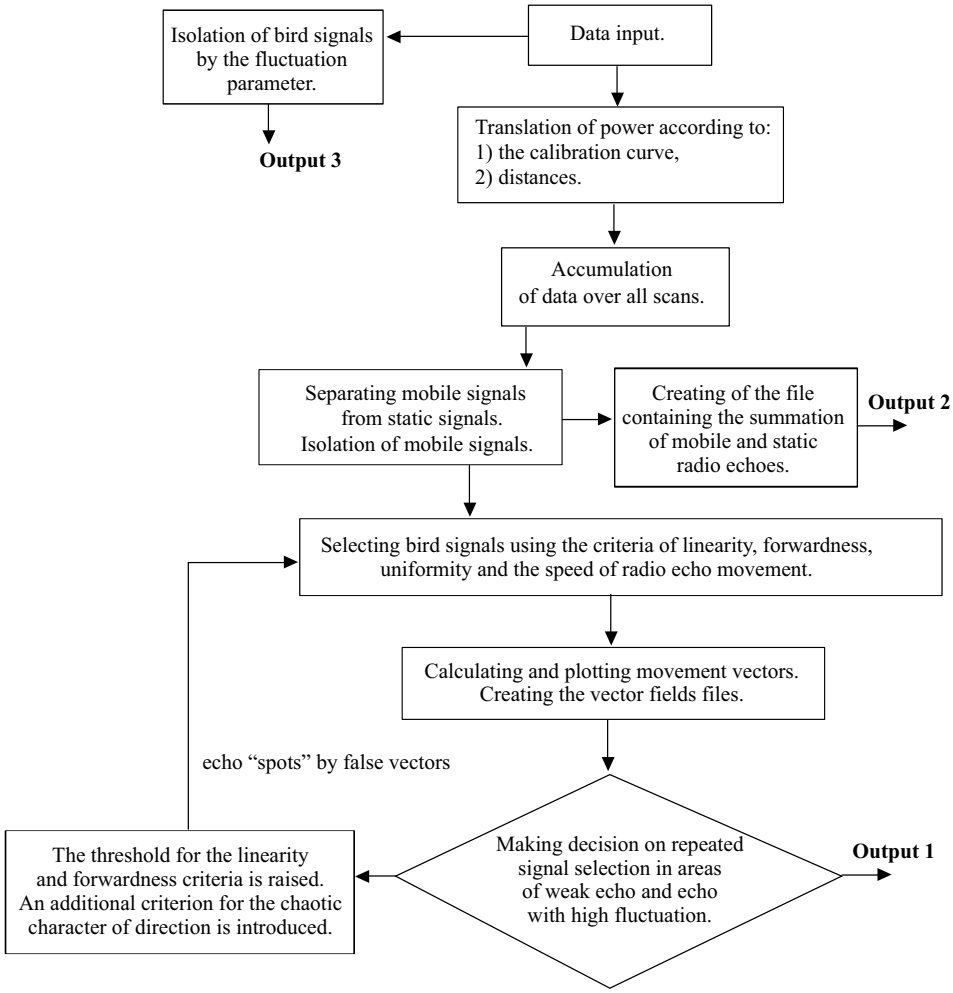

Fig. 3. The flowchart of the algorithm for bird identification and estimation of flight velocities

2. Isolating each bird (bird group) echo against echoes from other reflectors on the basis of echo movement and specific parameters of this movement.
3. Excluding false vectors by implementing a special analysis of vector fields on the basis of additional parameters.

Having completed the identification procedure, the algorithm plots ornithological and meteorological charts of various types.

METHOD AND ALGORITHM FOR SELECTING BIRD ECHOES

General considerations

As in the previously developed algorithm, the primary data used for selecting bird echo are reflectance fields obtained by summation of a preset number of successive scans performed at several tilt angles.

Based on the analysis of Table 5, we accepted the typical number of scans at each tilt angle to be eight. If this number is lower, part of useful information is lost. Increasing the number over eight does not yield an essential information gain, while increasing the computation time significantly.

Table 5
Comparison of computation time and data volume obtained over different number of scans (on the basis of 10 measurement cycles)

Number of scans	The quantity of identified birds (%)	Computation time (%)
7	70-90	80-90
8	**100**	**100**
9	100	120
10	100	150

These consideration underlie the first stage of selecting bird echoes at each point of each scan.

Stage 1

For each elevation angle value, radio-echo fields that were obtained over eight scans were summed up, and two data files were built.

The first data file contains charts plotted on the basis of summation of all the radio-echoes obtained during all the scans and at all the prescribed elevation angles (*Output 2* in Figure 3). These charts describe the total presence of all the targets under observation, as well as their movements in space. Figure 4 shows a sample of such a chart registering the situation at 12.56 *p.m.*, 8 October 2002; the radar is located in the centre of the chart. The upward direction is oriented northward; the scan radius is 60 km; the long line in the west marks the sea frontier. Bird echoes are represented by: (a) the streak of about 100 km long, southward-northward oriented; (b) the short southward oriented streaks in the east sector of the chart and (c) radio-echoes in the form of separate dots. This conclusion is supported by visual observations performed by a number of observers, the authors included, as the birds – Honey Buzzards (*Pernis apivorus*) – were flying right above the radar. Such streaks are frequently formed when birds are flying through a cloudless bottom mesofront layer caused by a breeze (Alpert *et al.* 2000). Convective flows thus formed create optimum routes for migrating birds (Leshem and Yom-Tov 1996).

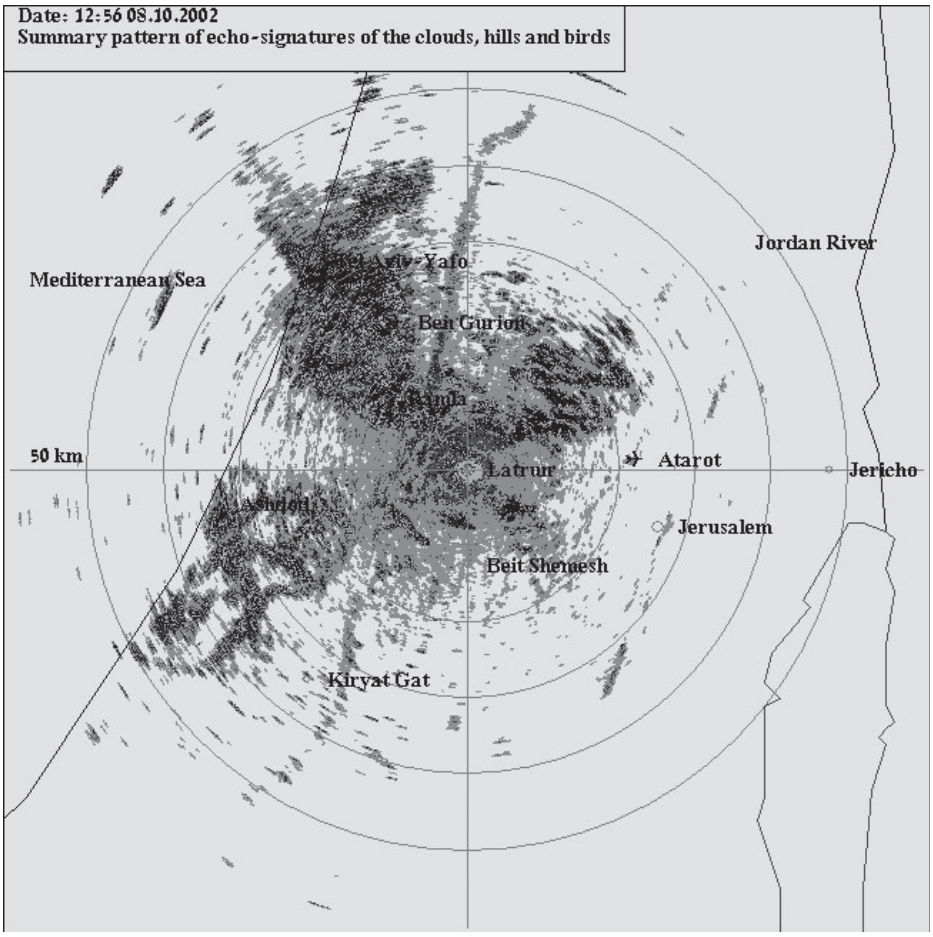

Fig. 4. Chart of summated radar echo at the level of the station sensitivity (8 Oct. 2002, 12.56 *p.m.*). 8 PPI were performed at each of the tilts of 0.5°, 2.0°, 3.5°, 5.0°, 6.5°, at the level of the station sensitivity. The chart presents the sum of all the echoes after digital processing of the data over all the PPI. The top part – direction towards the north. The firm line in the west is the sea-land border. The echoes in the form of "spots" of complicated shapes, as well as radial-orientated lines are reflections from ground clutter and objects in the sea; echoes in the form of a relatively straight line oriented from the north towards the south, which is about 100 km long, as well as short lines of similar direction and numerous dotted echoes represent birds.

Similar migration patterns of large flocks of various species, mostly storks, were observed by the authors every autumn and spring. Echoes in the form of areas, as well as of wide or narrow radial-oriented streaks and, in some cases, in the form of separate dots, are echoes reflected from ground clutter. These echoes change their configuration depending on refraction conditions. Using such charts for assessment of the ornithological situation implies a specific knowledge of the terrain, and the possibility of analysing echo evolution in time that can be done only by an experienced observer.

The second file contains data related to echo movements. Echoes registered at the same coordinate position more times than it is prescribed by a selected number (usually twice) are excluded from the further analysis. This procedure enables to exclude echoes from most of the ground clutter and of dense clouds.

The primary digital processing resulted in representing echoes in the form of "spots" formed by a number of signals (points), each point having its coordinates and power value (Dinevich *et al.* 2004). Taking into account the power values of the signals forming a particular "spot", the coordinate position of the centre for each "spot" is determined by the following dependencies:

$$\overline{X}c \quad \frac{\sum_{i}^{n} p_i x_i}{\sum_{i}^{n} p_i} \qquad \overline{Y}c \quad \frac{\sum_{i}^{n} p_i y_i}{\sum_{i}^{n} p_i}$$

where:

n – the number of signals (dots) forming the spot,
p_i – the power value of the signals,
i – the number of a dot within the "spot".

The upper value of i is restricted by the technical capabilities of a particular radar and the digital processing method, being 27 in our study. The low value of i is determined by the noise threshold, being i 4 in our study according to the measurements. At values $i < 4$, the number of echo "spots" multiplies by several factors, which significantly increases the computation time and eventually leads to a drop-in of false signals at the end of the filtering procedure. Clearly, this restriction leads to expulsion of some especially weak, but nevertheless relevant signals from further analysis. Evaluation of this error is beyond the framework of the present paper.

At *Stage 1*, as a result of the filtering procedure based on presence/absence of echo movement, a data file is obtained that contains the coordinates of the centres of "spots" representing echoes reflected from moving and/or heavily fluctuating objects. In certain weather conditions, such signals may be produced by echoes with considerable fluctuation, like those of atomized clouds, precipitation or some atmospheric heterogeneities, while mostly being echoes of flying birds.

Further filtering aimed at excluding non-bird echoes is based on specific properties of bird echo movement.

Stage 2

Additional considerations regarding the echoes from flying birds

As was shown above, the scattering cross-section of the same bird may vary significantly depending on the position of its wings and its orientation towards the radar. The calculations can be performed by means of the known equation for radiolocation of solitary target (Atlas 1964, Stepanenko 1973) in the following form:

$$R_{max} \left| \frac{P_t \quad G^2 \quad ^2 \quad K}{P_{min} \quad (4 \quad)^3} \right|^{\frac{1}{4}}$$

where:

P_t – the pulse radiation power,
G – the antenna gain,
λ – the radar wave length,
P_{min} – the receiver sensitivity,
σ – scattering cross-section
K – the radio-wave attenuation constant along the route of propagation.

Since technical parameters of MRL-5 and the conditions of wave propagation are known, this dependency can be solved for σ in case R_{max} value is known.

If we substitute P_{min} value for $P_0 = P_{min} \times 10^{0.1n}$, where n is the value of signal attenuation in dB and P_0 is the power of a target echo, we can calculate P_0 by measuring the actual values of R and n, assuming $K = 1$ and setting values for σ.

As can be seen from the equation, varying σ will lead to the corresponding variation, from scan to scan, of the power of P_0 echo or of the radar reflectance coefficient Z. At small values of σ, the echo power may be below the signal-detection threshold, *i.e.* be present in some of the scans while absent in other ones (see Fig. 1B, Fig. 2). Over subsequent scans, bird echo line can be both direct and broken (Ganja *et al.* 1991, Bruderer 1992).

In view of these considerations, the algorithm of additional bird echo selection based on specific movement properties implies performing the following three operations for each value of the tilt angle.

Operation #1: plotting straightforward echo movement segments by a prescribed number of points located within consecutive scans

The coordinate of the centre of each echo "spot" obtained in the first scan is assumed to be the point of origin for a coordinate system. Out of this central point, a bundle of n straight lines can be plotted. The end of each line should not be located beyond the distance that can be theoretically covered by a bird during the given time of observation (80 s, 8 scans in our case) in the range of minimum velocity V_{min} and maximum velocity V_{max}. The program enables to vary these parameters in the operational mode taking into account the actual velocities and wind directions.
Then:

$$L_{min} = V_{min} \times t \qquad L_{max} = V_{max} \times t$$

where:

L – the minimum/maximum distance that can be covered by a bird during the time between the first and the eight scan.

Any "spot" obtained in the scans that lies within this distance range is assumed to be the end of a straight line originating from each of the "spots" in the first scan. It is important to take into account that the initial echo from a bird may not necessarily appear within the first scan, but within any subsequent scan. In view of this

consideration, the procedure is repeated on the data obtained in the subsequent scans, assuming the centres of newly obtained "spots" to be points of origin for bundles of n lines. The procedure is repeated for scans 1-4.

Each of the n straight lines can be described by the dependency:

$$y = ax + b$$

where:

$a = (y_1 - y_2) / (x_1 - x_2)$,

$b = y_2 - ax_1$,

x_1, x_2, y_1, y_2 – the coordinates of echo "spots" in the first and the last scan, respectively.

In this coordinate system, the point of origin represents the location of the radar.

As a result of this procedure, a set of straight-line bundles is obtained, having their points of origins in the centres of echo "spots" that were registered for the first time.

At the next step, out of each bundle of n lines, the algorithm chooses m lines that meet certain requirements. Those are the lines on which not less than k signals are supposed to fall during the subsequent scans (k is a prescribed number, $k_{max} = 8$).

Operation #2: the movement uniformity criterion

Having obtained m straight lines plotted from each initially registered echo, we now select only those lines where the distance between the "spot" centres grows with each subsequent scan, *i.e.* $l_1 < l_2 < l_3 < l_n$, l_i being the distance between the "spot" centres obtained in two subsequent scans.

By the $l_1, l_2, \ldots l_n$ dependencies between subsequent scans, we can evaluate the uniformity of birds' flight velocities and set up certain values for the velocities that can serve as specific criteria. To do this, the system calculates the average bird velocity over the entire observation period and uses it as a benchmark to compare velocities within certain flight legs. In our study, the 20% value was chosen on the basis of multiple measurements. In case the deviation of flight velocity from the benchmark value is below 20% over at least one flight leg, the flight movement was considered to be a uniform one. In contrast, when the said deviation exceeded 20%, the movement was regarded as a non-uniformed one.

Operation #3: the movement linearity criterion

Among the set of lines that have remained within the analysis after *Operation #2* filtering, we now select the unique line where the diametral deviations of echo "spot" centres in consecutive scans are within a certain range of values prescribed by the linearity criterion. This value for a particular echo is assumed to be a certain prescribed length fraction of the direct line that connects the echo from the first scan to its "counterpart" in the last scan. The linearity criterion is fulfilled when the position of echo centres within the intermediate scans does not exceed this prescribed value. In our study, we set a 10% deviation to be the benchmark for the movement linearity criterion, namely, a deviation up to 10% of the line length means the movement is straightforward, while values from 10% to 40% characterize a non-straightforward movement. The problem is solved by selecting the maximum

proximity between a line and a set of echo centres obtained over a scan cycle. The required line is described by the dependency $y = ax + b$, where the coordinates of two points are known $(x_1, y_1; x_2, y_2)$, hence $a = (y_1 - y_2) / (x_1 - x_2)$; $b = y_2 - ax_1$, thus the problem is reduced to finding the minimum distance between the required "spots" (whose coordinates are known) and the preset line. To find those points, we drop a perpendicular from the point with coordinates (X_n, Y_n) on the said line; the coordinates of the base of this perpendicular being:

$$X_i \quad \frac{(X_n \quad aY_n \quad ab)}{1 \quad a_2} \qquad\qquad Y_i = aX_i + b$$

where:

X_i, Y_i – the coordinates of the point of intersection of the said line and the perpendicular dropped on it from the point X_n, Y_n.

Hence:

$$di \quad \sqrt{(X_n \quad x_i)^2 \quad (Y_n \quad y_i)^2}$$

where:

di – the distance between a point and the related line.

This distance should not exceed the value prescribed by the linearity criterion, thus:

$$di = (10 \div 40\%) \times L$$

where:

L – the distance between the echo centres in the first and the last scans.

There might be several perpendiculars meeting this requirement, out of which we choose the one which is the shortest for a given scan.

Therefore, only one line meeting the above-formulated requirements is chosen among all the lines originating from each initial echo "spot".

Stage 3 (isolating and excluding false lines)

The calculation of the state-of-chaos coefficient and making the correlated decisions is performed on the basis of the following procedures.

1. A control area is formed in form of a circle of a prescribed radius. The radius is set to be 600 m (the value determined experimentally).
2. The circle is subdivided into 8 sectors, which are numbered 1-8; number 1 is given to the sector with 0 direction that expands clockwise, number 2 is given to the adjacent sector clockwise, and so forth. Only dot-like echoes that serve as origins of direct lines are to be analysed.

The system automatically checks the orientation of line segments located within the control circle. It should be noted that the very technique of plotting the line segments indicates the direction of signals that form the said lines.

The decision-making algorithm obeys the following scheme:

1. The system determines the number of segments which, on the basis of their direction, were found within sectors 1-4. The total number of segments found in these sectors is calculated according to formula:

$$B_1 \quad \sum_{i}^{4} b_i$$

where:

i – *the number of a sector,*

b_i – the number of such segments.

2. The number b_j of segments found in sectors 5-8 is calculated – $B_2 = \sum_{j}^{4} b_j$.

3. The correlation coefficient is calculated as:

$$k_1 \quad \frac{\sum_{i}^{4} b_i}{\sum_{j}^{4} b_j}$$

At the next step, assuming the same echo being the centre of the control circle, the circle is turned clockwise, sector 1 now becoming sector 2 and so forth, thus shifting the 4-sector arrangement by one sector:

$$k_2 \quad \frac{(n_2 \quad n_3 \quad n_4 \quad n_5)}{(n_6 \quad n_7 \quad n_8 \quad n_1)}$$

In a similar way, k_3 and k_4 are calculated. Using the values k_1, k_2, k_3, k_4, the state-of-chaos coefficient is determined for K direction:

$$K \quad \frac{(k_1 \quad k_2 \quad k_3 \quad k_4)}{4}$$

If K is equal to 1, it indicates that the vectors throughout the control circle are oriented toward all the directions with equal probability, which is defined as a "state of chaos" incompatible with bird migratory flight pattern. The value of K in case of bird migration is to differ from unit as much as possible.

Hence, the system identifies vectors with $K = 1$ as false bird echo, but does not exclude them from the vector filed before the analysis of all the echo spots is completed. Only after calculating K values for all the vectors, the system establishes the areas of chaotic movement and excludes all the line segments plotted within these areas from the final data file. The n echo "spots" remaining after this operation are sent for a repeated procedure that calculates K value over $n + 1$ "spots". This calculation is performed on the basis of more complicated criteria. For example, if within the first cycle the lines were plotted for n "spots", within the second cycle this calculation is performed over $n + 1$ "spots" in the same area. The criteria for movement linearity and uniformity undergo similar complication.

DETERMINATION OF BIRD FLIGHT VELOCITIES AND PLOTTING FLIGHT VECTORS

As a result of *Stage 2* and *Stage 3* of filtering, straight-line segments are obtained, which are plotted over a prescribed number of echo "spot" centres that are moving within a given period of time. The technique used to plot this lines suggests that:

a) in case movement of an echo is represented by segments of lines meeting the above-described requirements, this echo belongs to a bird (bird group),
b) positions of echo centres in proximity to the general line which they form are determined by the flight pattern of a particular bird (bird group),
c) the orientation of lines relative to the coordinate system whose point of origin is the radar itself is considered to be the bird flight direction.

Having the coordinates of each vector and the time measurements corresponding to both its origin and terminus, we can calculate the average velocity of a bird (bird group) over the observation time. Having the coordinates of each echo centre and the exact time when the echo was first registered on the radar screen, we can establish the direction and the velocity of flight and determine whether the direction is or is not straightforward.

Using the values of X_i, Y_i, t_i, the root-mean-square linear regression dependencies $X(t)$, $Y(t)$ are built in the centres of the two echoes. The first echo centre is related to time t_1, the second point is related to time t_2, $t_2 > t_1$.

The slope ratios of the obtained dependencies X(t), $Y(t)$ provide evaluations of the bird's velocity components V_x and V_y. The actual bird (bird group) velocity is

$$\overset{\rho}{V}_{xy} \quad \sqrt{(v_x^2 \quad v_y^2)}$$

The averaged velocity of all the birds within the scanned area is assumed to be the mean velocity of bird migration flow $\overset{\rho}{V}_{sum}$ and is calculated as

$$\overset{\rho}{V}_{sum} \quad \frac{\overset{n}{\rho} \; \overset{\rho}{v}_{xy}}{n}$$

It is important to note that thus calculated radar-related bird flight velocity is, in fact, the sum of two components: a) the velocity of a bird's flight powered by its wing labour and b) the velocity and direction of the wind flow relative to the direction of the bird's flight.

The mean direction of bird migration flow is defined as the geometrical mean of all the flight vectors and is calculated by composition of vectors.

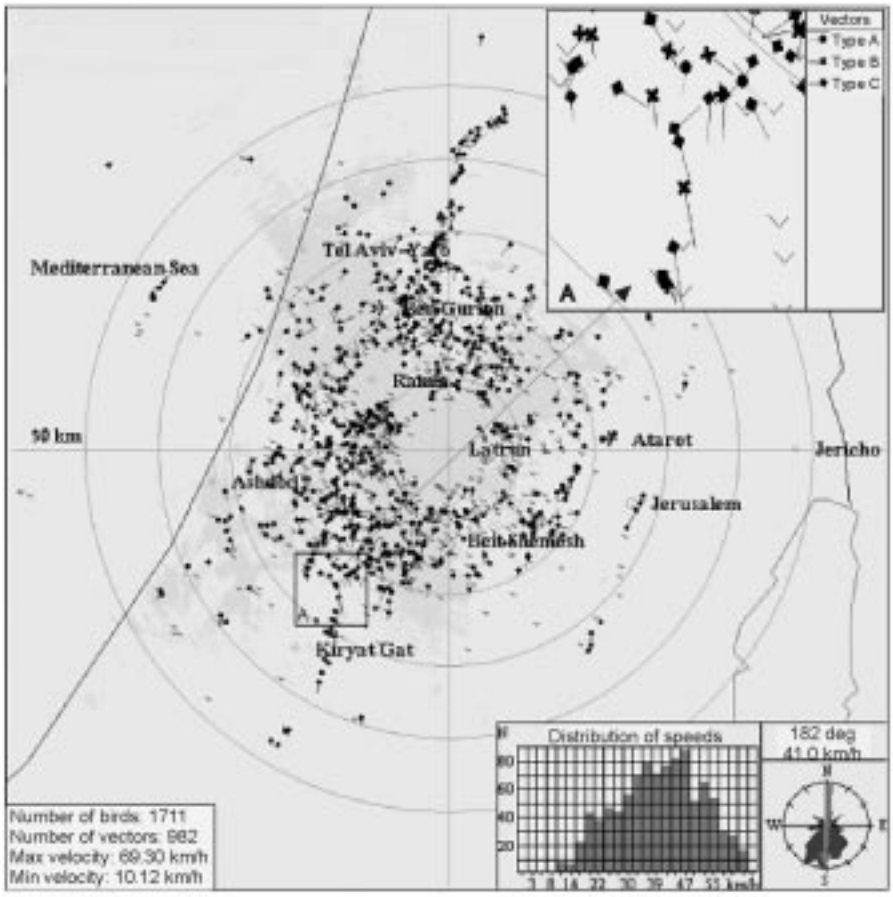

Fig. 5. Chart of summated radar echo (Fig. 4) after selection of bird signals and plotting their movements in the vector form (Ornithological chart).
Section A – an enlarged fragment of the vector field. Symbols put at the origin of a vector designate: v – movement with frequently changing direction; ● – straightforward and even movement; × – straightforward, but uneven movement; ◆ – movement with considerable deviations from straight line and uneven in its speed.
On the right below: two distributions containing: 1) the speed spectrum and 2) the direction spectrum.
On the left below: the general quantity of birds, including those with directional movement, and data reflecting the maximum and the minimum speed values.

GRAPHIC REPRESENTATION OF BIRD FLIGHT DATA AGAINST THE BACKGROUND OF GROUND CLUTTER AND ATMOSPHERIC INHOMOGENEITIES

Upon completing all the stages of echo filtering, a file containing only bird-related data is obtained. After summation of the totality of the data over all the scan angles, we obtain a sum horizontal plane projection of all the vectors that

represent flights of all the birds within the scanned area. If we then chart scale cursors, residence sites, roads, the coastline and other terrain elements on the said projection, we obtain a chart that can be called a radar ornithological chart (by analogy with a weather chart).

A sample of such a chart is presented in Figure 5 (data obtained at 12.56 *p.m.*, 8 October 2002). The chart presents the same ornithological situation as that in Figure 4 after the algorithm has performed the filtering procedure.

As can be seen, the volume of information in Figure 5 is significantly larger than that in Figure 4. Bird echoes are presented in a vector form. The scan radius is 60 km. The length of the band representing migrating birds is about 100 km and consists of segments differing in vector density. The total quantity of birds (bird groups) is 1711, among them 982 are flying with steady direction, as is demonstrated by the corresponding vectors.

The flight velocity spectra show that the maximum bird velocity (taking into account the wind velocity) is about 70 km/h, while the minimum velocity is just over 10 km/h. As can be seen from the direction rose, the sum vector is oriented pronouncedly toward the south (182). The four above-mentioned patterns of echo movement are actually plotted in different colours, but in the monochromatic image in Figure 5 the colours are substituted for designating symbols shown in the framed scaled-up A section.

The same sum database is used for plotting the graph of birds' distribution over height within a prescribed scanned area. A sample of such a chart is shown in Figure 6, where the *X*-axis indicates the quantity of birds (bird groups) and the *Y*-axis indicates the height.

There are several paired bars in the graph. The length of each bar is proportionate to the number of birds within the corresponding 500 m high layer. The bottom bar in a pair is the number of birds that fly with frequently changing directions, *i.e.* non-migrating birds; the upper bar in a pair is the number of birds whose flight vectors have been plotted by the algorithm, *i.e.* migrating birds.

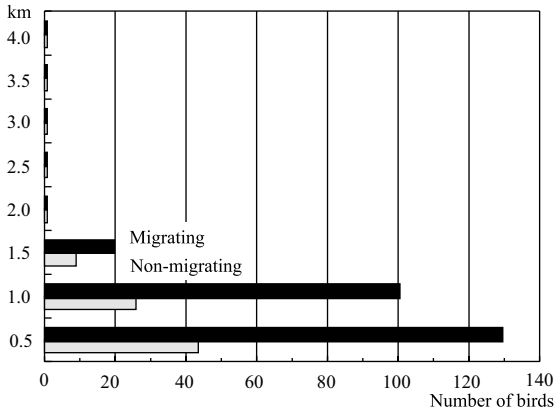

Fig. 6. Distribution of migrating and non-migrating birds at different heights (data from Figure 5)

Figure 7 shows a sample of volume visualisation of bird distribution over certain terrain areas. The arrow taken out of the drawing indicates the northward orientation; the large dot indicates the position of the radar. In the west, the terrain changes into the coastline, in the east there are hills. The horizontal planes are positioned at different heights.

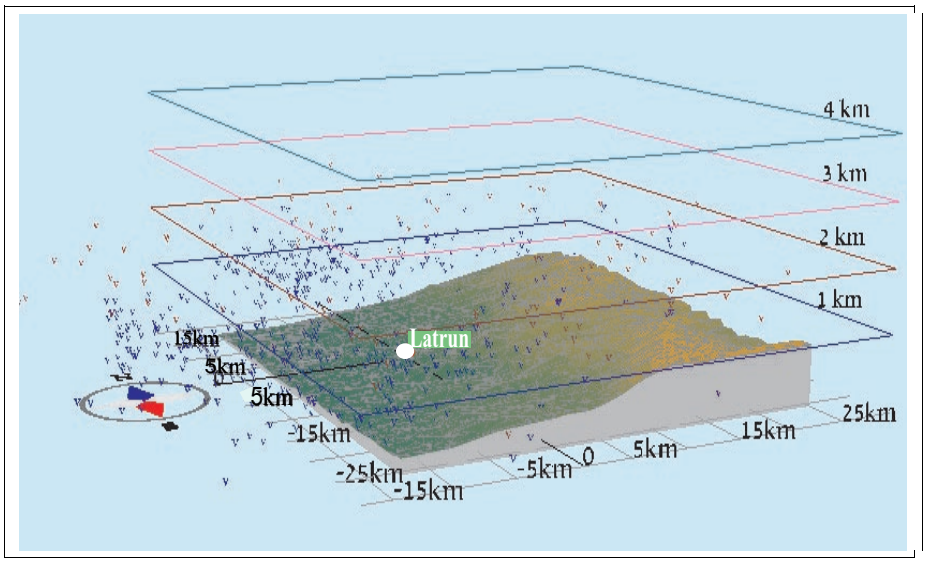

Fig. 7. A sample of volume visualisation of the birds distribution.
The radar is located at the intersection $x = 0, y = 0$. The horizontal planes are drawn at the heights of 1, 2, 3 and 4 km. The arrow is northward oriented. The sea is in the west, in the east there are hills. The dotted echoes represent birds. The program allows to view this picture at various angles and at various scales, to determine the coordinates of each radar echo.

The proposed algorithm provides on-line determination of the exact coordinate position of each bird echo. The databases constituting the two abovementioned files (see *Stage 1*) make it possible to superpose ornithological and meteorological data and to obtain combined charts that provide the bird monitoring data (in a vector form) simultaneously with the data on ground clutter and atmospheric inhomogeneities.

Figure 8 shows a sample of a combined chart obtained at 8.20 *a.m.*, 21 October 2002 and Figure 9 – relevant heights distribution (analogous to Figure 6). For the sake of comparison, Figure 10 shows the corresponding chart showing radio-echoes after *Stage 1* of the filtering procedure, *i.e.* echoes selected by the movement characteristic alone, without the subsequent filtering accurately identifying bird echoes.

Figure 8 presents a finalised chart based on the data obtained throughout all the stages of the above described filtering procedure. It contains a vast corpus of various data demonstrating the advantages of the proposed algorithm, as can be seen below:

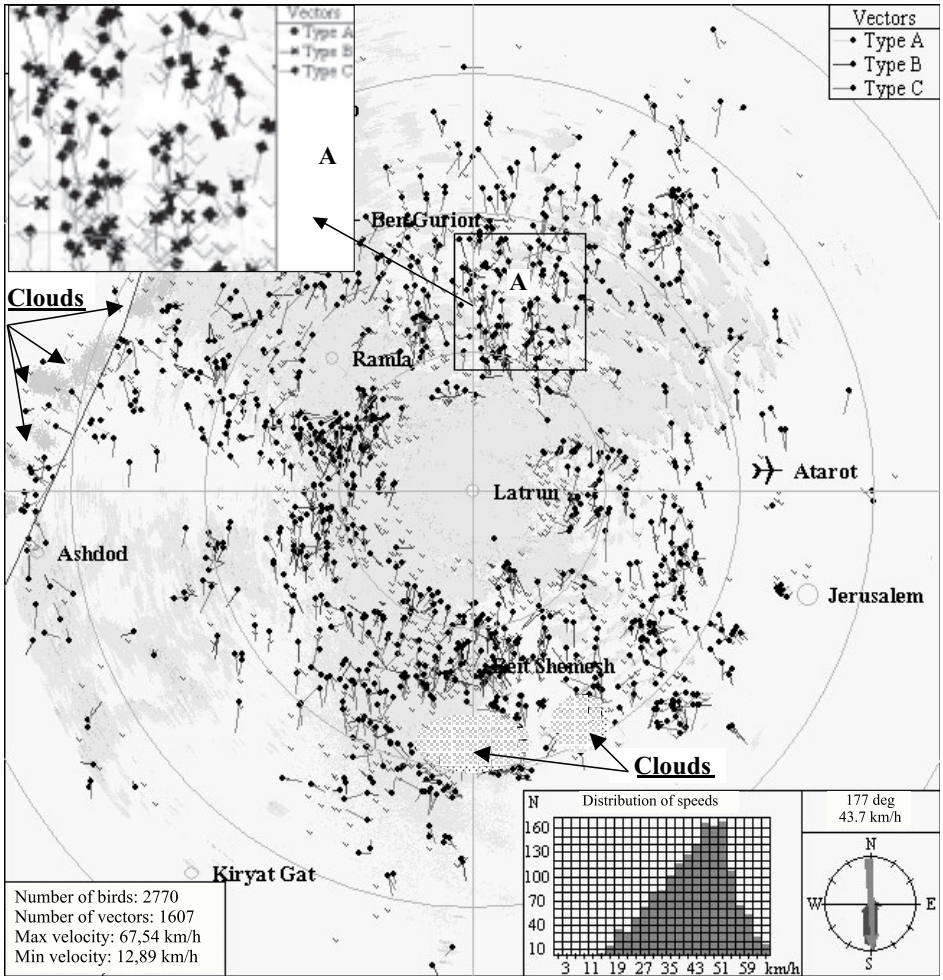

Fig. 8. Ornithological chart against the background of ground clutter and atmospheric formations (21 Oct. 2002, 8.20 *a.m.*). Echoes in vector form – migrating birds; echoes in tick form – local birds; echoes in form of shapeless vague areals – ground clutter; echoes in form of shaded domains – clouds and precipitation. Fragment A with enlarged vectors is isolated and presented in the top left corner for the sake of illustration. In the southern sector of the chart, one can see a bird flow between two cloud cells. Other explanations as in Fig. 5.
On the coloured charts, different types of radar echo, as well as vectors characterizing different patterns of movement, are marked with various colours: (echoes from ground clutter are marked with green, echoes from clouds and precipitation with blue, and the three types of vectors are marked with red, dark blue and brown).

a) Total quantity of bird echo within 30 km radius from the radar is 2770 (charts can be plotted up to 60 km radius).
b) Number of vectors (*i.e.* birds flying in distinct direction) is 1670.
c) Maximum radar-related echo movement velocity is approximately 68 km/h; minimum radar-related echo movement velocity is approximately 13 km/h.

d) The majority of birds fly at 45-50 km/h velocity.
e) Average flight velocity is 44 km/h.

Most of the birds fly at varying velocity, deviating from a straight line; however, there is a significant number of echo that deviate from a straight line but move at uniform velocity.

Within the scanned area, one can distinguish bird groups differing in concentration.

Birds tend to by-pass clouds, flying around the perimeter or "diving" into gaps between separate cloud cells (as can be seen in the area occupied by two cloud cells in the southern part of the chart).

Within 180-270 sector (Fig. 9), the maximum bird echo concentration is observed in the 0-500 m high layer (209 bird groups); a significant number of echo from birds flying within the 500-1000 m layer (150 bird groups); a small number of bird groups were observed within 1000-3000 m height, only 13 bird groups were registered at heights of 2000-3000 m.

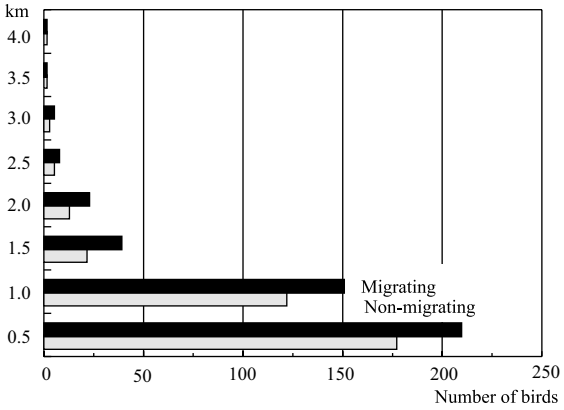

Fig. 9. Distribution of migrating and non-migrating birds at different heights (data from Figure 8)

Preferred flight direction is 177 , while there are a small number of echo from birds flying in the reverse direction. The latter phenomenon has been observed in a number of studies (Komenda-Zehnder *et al.* 2002).

All the data can be obtained from the scanning of the whole horizon (360°) every 10-15 minutes and delivered to users on-line. It is noteworthy that the described charts provide only the general information on atmospheric inhomogeneities, namely, their location and shift dynamics. More complete data on clouds, precipitation *etc.* is provided by radar meteorological charts of a different type. The proposed algorithm plots these charts in parallel with the ornithological charts, while radar data for the former charts are collected by means of a specifically designed software. Within this task, one of the conditions for data collection is antenna elevation up to 85°.

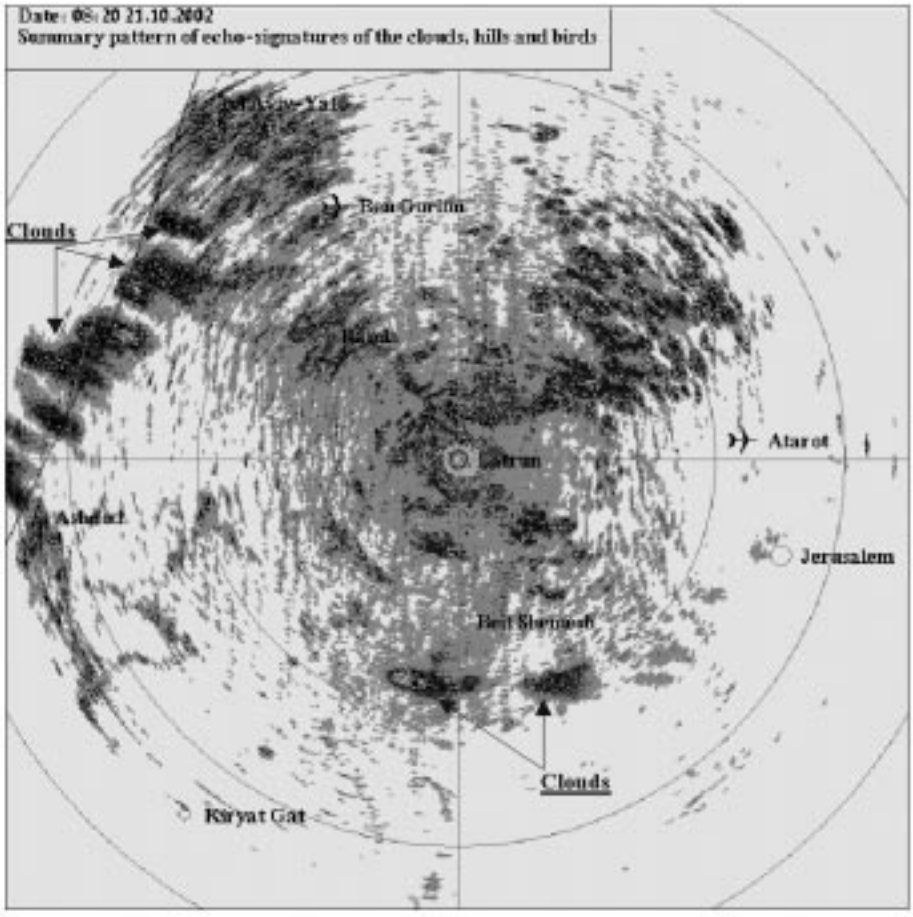

Fig. 10. Chart of summed radar echo. Comparison of Figure 8 and 10 enables to classify the echo on the chart by types of reflecting objects. Arrows indicate the zones of radio echo from clouds; radio echo in the form of spots, radial-orientated lines presents local objects; dotted lines present southward orientation, firm lines in the near-by zone indicate bird movement. In the southern sector one can see dotted bird echoes located between two cloud cells.

PROBABILITIES OF DETECTING BIRDS WITHIN DIFFERENT RANGES FROM THE RADAR

The probabilities of detecting birds within different ranges from the radar can be established by analysing the data presented in Tables 6a and 6b. In the numerators, there are mean values for the amount of bird echo per unit of area (n_{cp}), that were photo-registered on the screen of circular scan indicator. These data were obtained within different ranges from the radar. In the denominators, there are values of probability (P) at which birds can be detected within those ranges. P = 100% is

the amount of bird echo observed at the distance from the radar (ΔR) from 5 to 10 km. Values of P for other distances were calculated in relation to ΔR. In each ΔR_i area, the number n_i of bird echo was recalculated per unit of area. It enables to obtain n_i for each selected distance ranges within the radius of 60 km from the radar.

To assess the probability of bird detecting with the help of MRL-5 radar, we analysed observation data collected during intensive bird migration in November 2000 (night-time from 10.00 *p.m.* to 1.00 *a.m.*, see Table 6a; daytime from 12.00 to 1.00 *p.m.*, see Table 6b). Sample of migration charts are given in Figure 5 and 8. The intensity of migration was determined by radar data and observations made by the ornithologists.

Table 6a
Dependency of bird echo (n_{cp}) detected at different distances at night, at λ = 10 cm

	Distance to the radar (km)					
	5-10	10-20	20-30	30-40	40-50	50-60
n_{cp} / P (%)	28.5 / 100	27.0 / 95	25.4 / 89	14.7 / 52	10.9 / 38	6.0 / 21
	29.2 / 100	25.8 / 88	24.2 / 83	12.3 / 42	11.5 / 39	5.1 / 17
	17.8 / 100	15.9 / 89	13.2 / 74	8.5 / 48	7.3 / 41	4.1 / 23
	16.9 / 100	14.5 / 86	12.8 / 76	6.5 / 38	3.2 / 19	-
	24.3 / 100	25.5 / 100	20.3 / 84	8.6 / 35	3.3 / 14	-
Birds in % ΔP (%)	**100**	**86-100**	**74-89**	**35-52**	**14-41**	**~20**

Table 6b
Dependency of bird echo (n_{cp}) detected at different distances in the daytime, at λ = 10 cm

	Distance to the radar (km)					
	5-10	10-20	20-30	30-40	40-50	50-60
n_{cp} / P (%)	64.9 / 100	65.0 / 100	58.0 / 89	49.0 / 75	510 / 79	46.0 / 71
	25.6 / 100	23.7 / 93	19.8 / 77	22.0 / 86	21.0 / 82	17.4 / 68
	48.0 / 100	46.5 / 98	37.6 / 78	35.7 / 74	37.3 / 78	38.4 / 80
	17.9 / 100	17.2 / 100	148 / 83	12.4 / 69	13.5 / 75	13.0 / 73
	83.4 / 100	79.5 / 95	74.2 / 89	56.8 / 68	51.3 / 61	47.0 / 56
	17.0 / 100	16.5 / 97	15.2 / 89	13.1 / 77	12.9 / 76	10.2 / 60
***Birds in* % ΔP (%)**	**100**	**93-100**	**77-89**	**68-86**	**61-82**	**56-83**

Long-term radar observations suggest that during seasonal migrations flying bird can spread over large spaces at almost uniform density. At night the density is uniform over the radar scanning areas, while in the daytime this uniformity is observed along certain azimuth sectors. It may be assumed that bird species and their sizes are uniform over a large space for each given moment of measurements. Hence, the dependence of the number of bird echo on the distance can be considered as the function of the radar potential entirely.

Under these conditions, photos were chosen for data analysis (similar to those in Fig. 1B) that were made off the radar screen during horizontal scans in the period of especially intensive bird migration. The scans were performed at tilts not less that 3 , when the number of ground clutter echo and the impact of lateral lobes are significantly lower.

As is seen in Table 6: (a) at distances up to 30 km, MRL-5 radar detects birds with probability of about 80%, (b) at up to 40 km, the probability of detecting birds is not less that 35-52%, (c) at longer distances, the probability drops significantly. It should be noted that in some cases larger birds flying at night can be detected with high probability at distances up to 40 km.

Daytime bird migrants usually fly in streaks oriented along the coastline. In autumn and spring the flight directions are almost reverse. Daytime migrants (*e.g.* storks, pelicans, eagles, buzzards, *etc.*) are usually of larger size than the night-time ones. They take advantage of convective atmospheric streams formed by uneven ground surface, as well as by valley-mountain and breeze factors. Reflectivity (Z) of daytime migrants is much higher that that of smaller night-time birds. The streaks often reach 100-120 km in length. The analysis of the daytime observation data shows that MRL-5 detects not less than 80% of birds at the distances up to 30 km, which is close to detection level of night-time birds (Table 6b). At distances up to 60 km, the radar detects not less than 60% birds, which exceeds the level of night-time detection.

It should be noted that MRL-5 is able to register echo of birds as large as storks with high trustworthiness at distances up to 90 km. The present paper deals with a system capable of selecting bird echo and plotting ornithological charts within distances up to 60 km, mainly due to computation speed limitations, a vast corpus of complex data and the necessity to update the charts for air traffic control every 10-15 minutes.

TESTING THE METHOD AND ANALYSING THE RESULTS

The first testing technique

In order to test the method for identifying bird echoes suggested in the study, a comparison analogue was to be implemented that yield data which can be regarded as trustworthy. The method for identifying bird echo by means of photographing the radar screen was chosen as such. A sample of bird echo identification by means of this method is shown in Figures 1 (A, B) and 2.

Comparing these photos enables to identify bird echo with high accuracy, the error depending entirely on the quality of photography. Therefore, comparing the data on the amount of birds obtained by means of photography with those obtained by computerised echo selection, we can assess the relative error and compare the calculated velocities of birds' movements. To do so, it is enough to randomly select a certain number of tracks and calculate their length. By calculating

the ratio of a track length to the exposure time, we obtain the mean flight velocity. However, one cannot expect the data coincide completely, due to a number of reasons. First, there is a time shift of 3-5 min between the two modes of observation. Second, the calculation of the number of birds on a photo is performed manually as opposed to the digital analysis. Third, photo representation of the radar screen depends on the quality of photography.

An example is given below of bird echo identification by means of the proposed algorithm in comparison with the photo-based method. The data were obtained and processed by the algorithm at 8.30 *a.m.* and 9.15 *a.m.*, on 21 October 2002, at two tilts (1.0 and 3.0). At the same tilts, with a time interval of 3-5 min, the corresponding echoes were photographed (see results in Table 7). There is a relative agreement between the data obtained by the two techniques, which suggests that the proposed algorithm identifies bird echo with high confidence. The total time required for the algorithm to identify bird echoes according to all the criteria described above, to calculate flight vectors and to plot different kinds of ornithological charts does not exceed 15 min. The calculation time can be reduced by using a higher-speed computer.

Table 7
Comparison of data on the number of birds and their flight velocities obtained by the computerised signal processing system *vs* photographic registration

Type of data	First test, 8.30 *a.m.*		Second test, 9.15 *a.m.*	
Technique of selection	Computerised	Photographic	Computerised	Photographic
Number of birds	1285	1154	194	153
Maximum velocity (km/h)	65.3	59.4	46.4	43.0
Minimum velocity (km/h)	12.2	10.3	11.6	11.2
Mean velocity (km/h)	40.5	38.5	35.3	35.7

The second testing technique

A special analytic software enables to trace the movement of echo “spots” in time, making it possible to reproduce all the stages of plotting each single vector and the entire vector field. Below, a sample of such analysis is given.

Figure 11 shows a comprehensive ornithological chart in the form of a vector field plotted on 29 August 2003, when a large stork flock flew over Israel. The length of the bird band exceeds 100 km. The small square in the southern sector of the chart presents a sample framed for more detailed analysis, chosen for the sake of simplicity as it contains only two vectors. The large framed square in Figure 12 presents those two vectors together with echo “spots” whose centres were used to plot them. The calculated echo centres are marked with dots. The point at the origin of each vector coincides with the centre of the initially registered “spot”, *i.e.* with the moment the bird was first registered in the given observation series. The

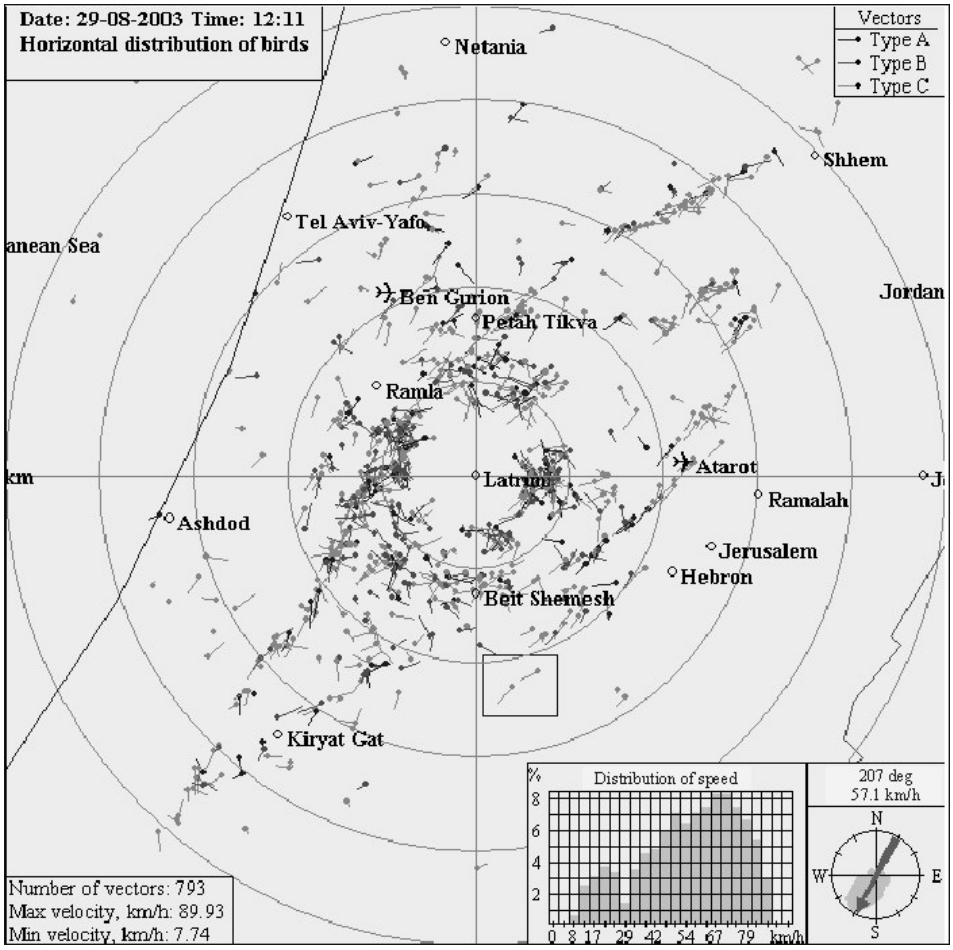

Fig. 11. Analysis of plotting bird flight vectors. Ornithological chart obtained at 12.11 *p.m*., 29 Aug. 2003. All the designations are similar to those in the previous figures; scan radius – 50 km. The 100 km long echo streak in form of vectors oriented from the south to the north, as well as separate short streaks are echoes of storks. According to visual observations performed by several observers both in the proximity to the radar and at a distance, the stork were flying at the height of 200-400 m; duration of the observations – about 3 hours. The square is the target area for the analysis shown in the next figure. Other explanations as in Figure 5.

length of a vector is proportionate to the flight velocity. Squares 1-6 in Figure 12 show the dynamics of these echo movement from scan to scan. The first (northern) vector was plotted over five echo "spots" that were moving uniformly but not straightforwardly. It disappeared in the third scan, being apparently below the noise level. The movement of this bird (bird group) is straightforward but not uniform velocity-wise. The second (southern) vector is plotted over six echo "spots" moving uniformly from scan to scan. The movement of this bird (bird group) is uniform but not straightforward.

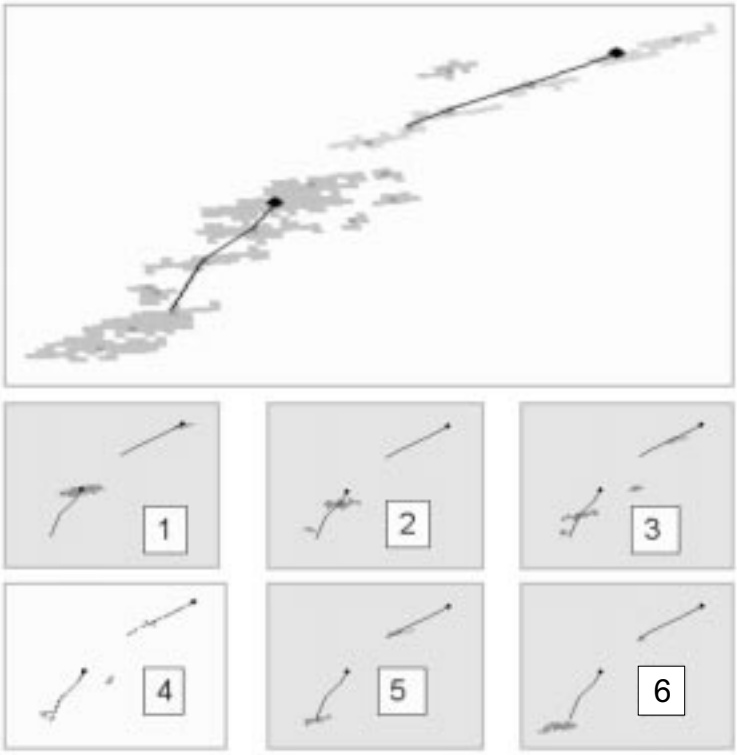

Fig. 12. The course of analysis in the enlarged area from Figure 11* of succesive scans. The dynamics of echo "spots" movements in time (from scan to scan) is shown in the from of two vectors plotted by centres of the echo "spots". 6 out of 8 scans are presented. Echoes from these groups of birds were not found within scans 7 and 8.

Analysis of this kind enables to assess the impact of every parameter included into the algorithm for bird echo selection at every stage of the procedure and to search for the optimum values of these parameters.

The third testing technique

Parallel comparative observations over the storks were performed both with the help of the radar and by visual observers on board a plane. The plane was directed in on-line mode to the area of birds' migration following the position data provided by the radar. Direct radio contact was maintained between the observer onboard and the radar operator. Conducting an experiment of this kind is complicated by the fact that it is not always possible to overlap in time the target area of the radar observation and the plane. The main difficulty is caused by the high density of aircraft in the air and the limitations imposed on the area where a research plane might fly at variable height profile. Nevertheless, in all the cases when it was possible to have the plane within the area and at the height of bird echo, according to the position data of provided by the radar, the onboard observer could see the storks, keeping the plane route parallel to that of the birds.

* Numbers 1-6 represent

SOME PROSPECTS FOR FURTHER DEVELOPMENT AND INCREASING THE RELIABILITY OF THE SYSTEM

Weak echoes with pronounced fluctuation, such as echoes from atomized clouds and precipitation, as well as from insects and atmospheric inhomogeneities, pose a major problem for the algorithm. In order to achieve more reliable identification of such echoes, the system based on MRL-5 will be able in future to use several additional properties, among them:

a) The ratio of echo power on the two wave lengths. The ratio of echo power on the two wave lengths depends entirely on the properties of the target (Abshayev *et al.* 1980). It has been shown in several studies (Glover and Hardy 1966, Hajovsky *et al.* 1966, Chernikov 1979) that power of echo reflected from insects on 3 cm wave is higher that that on 10 cm wave. In case of bird echo, this ratio is inverse. The same ratio characterizes echoes from atomized clouds and precipitation (Atlas 1964, Stepanenko 1973). Therefore, the ratio of reflection coefficients on the two wave lengths ($Z_{dBZ3cm} / Z_{dBZ10cm} > 1$ – not birds) may serve as an additional characteristic for identifying bird echoes and eliminating false vectors.

b) Polarization characteristics of echo. A polarization devise specially developed for MRL-5 enables to vary radiation polarization per pulse on 3 cm wave length and hence to receive a signal of polarization identical to this of the pulse; in addition, it enables to obtain their depolarization components (Dinevich *et al.* 1994). On the basis of the depolarization components, it is possible to calculate the value of depolarization ΔP and the value of differential polarization dP, which are functions of nonsphericity and orientation of nonspherical targets in space (Chernikov and Schupjatsky 1967, Lofgren and Battan 1969, Zrnic and Ryzhkov 1998). The measurements we have performed in Israel show that the degree of depolarization of bird echoes is about $\Delta P = -7 \div -10$ dB, while the value of differential polarization is $dP >> 1$. These data are in good agreement with those obtained elsewhere (Chernikov and Schupjatsky 1967). Taking into account that small drops in clouds and precipitation are spherical in shape, their dP value is close to unity (Schupjatsky 1959). These criteria can become an important parameter for increasing the reliability of identifying birds against the background of highly fluctuating echo reflected from atomized clouds and precipitation.

c) Fluctuation characteristics of echoes from different targets. On the basis of our analysis of fluctuation characteristics of echoes from different targets (Dinevich *et al.* 2004), a special device was designed. It enables to isolate the signal of maximum amplitude within each reflected monitoring pulse, within a preset 200 m long strobe and the antenna being on halt. Isolated signals are stored and accumulated, to be used by a special software for plotting amplitude and frequency spectra over 10-15 s samples. Taking into account the recurrence of monitoring pulses in MRL-5 (500 pulses per second), for each sample a power variance spectrum is formed for 5000 and 10 000 signals. These data is used to calculate frequency spectra typical of dif-

ferent targets. A specially designed low-frequency filter made it possible to classify the spectra of peak fluctuation into two categories ("bird"/"non bird") at the accuracy of at least 80% (Fig. 13). In case when the signal is reflected from a single bird, the accuracy of target identification is over 95%. Figure 14 shows a sample of results obtained by means of the filter for typical echo spectra.

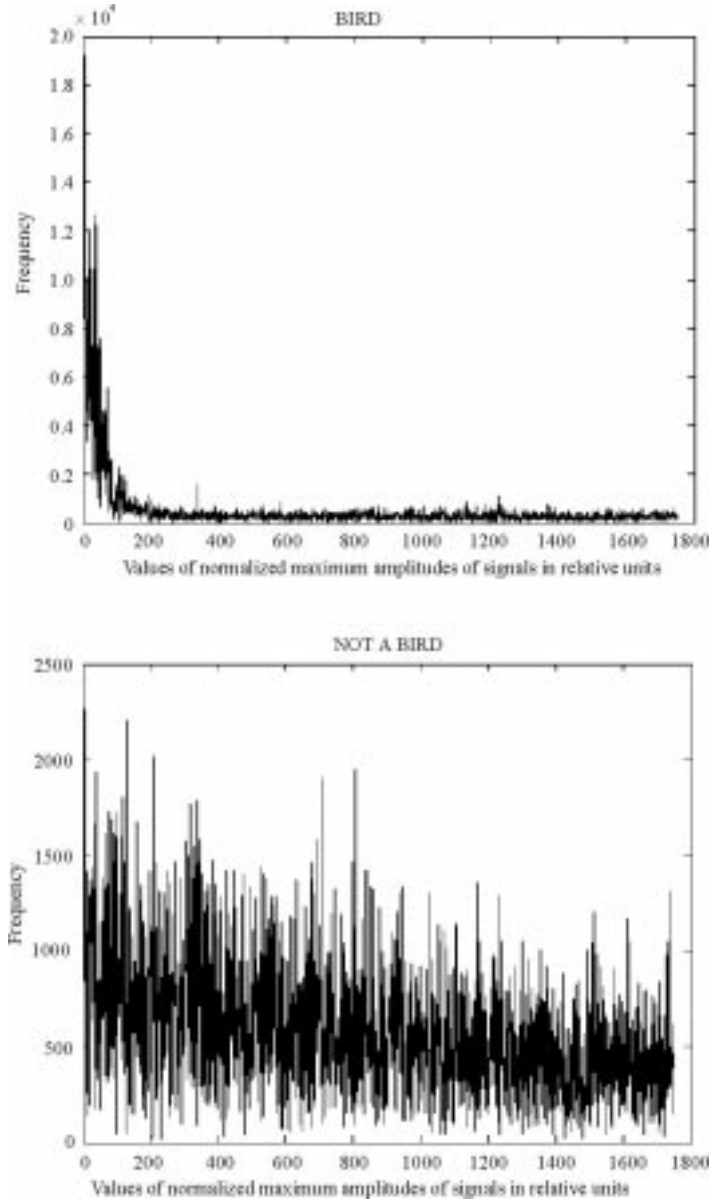

Fig. 13. Typical frequency spectra of signals from birds and non-birds. *X*-axis – signal frequency (in relative units); *Y*-axis – the frequency of recurrence of normalized maximums of signal amplitudes (in relative units).

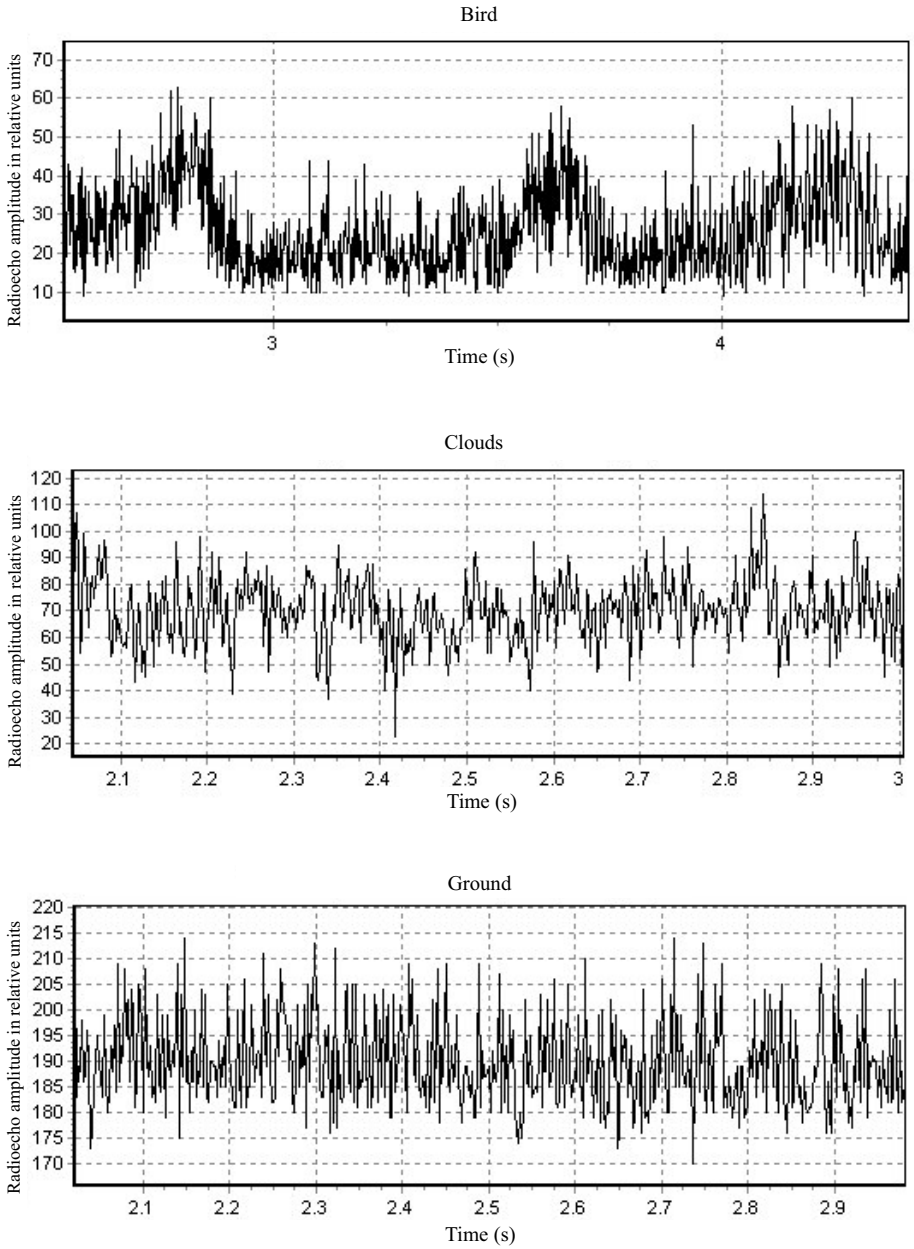

Fig. 14. Characteristic oscillographs of echoes reflected from birds, clouds and ground clutter. The *X*-axis shows time of signal accumulation, the *Y*-axis shows the signal amplitude in relative units.

d) Using the algorithm in Doppler radars. In case radar echo mobility is determined by measuring its Doppler frequency shift (Doviak and Zrnic 1984), the first procedure can be excluded from the proposed algorithm. Using the rest of the procedures and properties for plotting vectors, one can obtain ornithological charts

described above. The network for ornithological radar monitoring (Leshem and Gauthreaux 1996) may then include most of European radar stations (see Table 8). As can be seen, over 70% of meteorological radars in Europe use the 5.3 cm band and are able to measure the Doppler component of echo frequency. Countries hosting such stations participate in OPERA project aimed at exchange of radar data.

Table 8
Countries participating in the OPERA (*Operational Program of the Exchange of Weather Radar Information*) program at exchanging radar information

	Country	VMO Code	Number of operational MRL	Number of MRL in project	Bandwidth of MRL
1	Austria	OS	4	0	CD
2	Belgium	BX	1	1	CD
3	Bulgaria	BU	3	0	CD **+ 2X/S**
4	Great Britain	UK	13	0	2CD **+ 11C**
5	Hungary	HU	3	0	CD **+2X/S**
6	Germany	DL	15	1	CD
7	Greece	GR	4	0	**?**
8	Denmark	DN	3	0	CD
9	Ireland	IE	2	0	CD
10	Island	IL	1	0	**C**
11	Spain	SR	13	2	14CD +1SD
12	Italy	IY	10	6	13CD+1SD+**2C**
13	Latvia	LV	1	0	**X/S**
14	The Netherlands	NL	2	0	CD
15	Norway	NO	2	1	CD
16	Poland	PL	3	4	2 CD **+X/S**
17	Portugal	PO	2	1	CD
18	Romania	RO	1	0	**?**
19	Slovakia	SQ	2	0	CD **+X/S**
20	Slovenia	IJ	1	1	CD
21	Finland	FI	7	0	CD
22	France	FR	15	5	12C **+ 8S**
23	Croatia	RH	3	0	**S**
24	Czechia	CZ	2	1	CD
25	Switzerland	SW	3	0	CD
26	Sweden	SN	12	0	CD
27	Estonia	EO	1	1	CD
	Total		**128**	**24**	

Explanations of symbols: D – Doppler; NMRL – incoherent meteorological radar station; DMRL – Doppler meteorological radar station

Bandwidth	Wave length (cm)	Type of MRL
C	5.3	NMRL
CD	5.3	**DMRL**
S	10	NMRL
SD	10	**DMRL**
X/S	3/10	NMRL

CONCLUSIONS

1. The study enabled to establish a set of radar characteristics and on this basis to develop an algorithm that enables to distinguish bird echo and perform on-line plotting of vector fields that represent birds' movement, including the height parameters.
2. The technique of vector field plotting enables to classify birds, on the basis of their movement patterns, into four categories, among them birds flying with frequent shifts in flight direction (local birds), birds flying straightforwardly at steady velocity or at varying velocity, and those flying with repeating deviation from a straight line and at variable velocity.
3. Comprehensive charts plotted on the basis of the algorithm data enable to obtain diverse and relevant information on the ornithological situation within the area of 60 km radius from the radar position, including:
   – the total current quantity of birds in the air, specifically migrating birds,
   – maximum and minimum flight velocity values,
   – distribution of birds' mass throughout the height,
   – the spectra of flight directions and velocities, including the sum direction vector,
   – vector fields of bird movement juxtaposed with current meteorological status and local terrain,
   – bird distribution by the flight pattern (the degree of straightforwardness and velocity steadiness),
   – data on clouds, precipitation and visually unobservable atmospheric inhomogeneities, including their evolution with time.
4. Weak echoes with pronounced fluctuation, such as echoes from atomized clouds and precipitation, as well as from insects and atmospheric inhomogeneities, pose a major problem for the algorithm. However, in future the system will enable to apply additional properties, which will increase the identification reliability of echo of this type. Among the properties mentioned, there is the ratio of reflection coefficients on the two wave lengths, as well as polarization and fluctuation parameters of echoes obtained from various targets.
5. The radar ornithological system described in the paper enables to perform real-time monitoring of global intercontinental migrations of large bird flocks by means of the network of radars, among them MRL-5, located in different countries and covering vast territories.
6. The method of bird identification proposed in the study can be implemented in other types of high-grade potential coherent and incoherent radars whose antennas produce narrow-directivity beams.

ACKNOWLEDGEMENTS

The authors express their gratitude to the Ministry of Defence of Israel for financing the project; to the Ministry of Immigrant Absorption for financing the KAMEA program; to the administration of the University of Tel Aviv for their constant assistance. Our thanks go to A. Kapitannikov, O. Sikora, Dr M. Pinsky and Dr. A. Sterkin for their assistance in fulfilling a number of project tasks; to V. Garanin, D. Stilvelman and V. Dinevich for providing radar maintenance.

REFERENCES

Abshayev M., Burtsev I., Vaksenburg S., Shevela G. 1980. [*Guide for use of the MRL-4, MRL-5 and MRL-6 radars in urban protection systems*.] Hydrometeoizdat, Leningrad. (In Russian).

Abshayev M., Kaplan L., Kapitannikov A. 1984. [*Form reflection of meteorologic targets at the primary processing of the meteorologic radar signal*.] Transactions of VGI 55. (In Russian).

Alpert P., Tannhauser D.S., Leshem Y., Kravitz A., Rabinovitch-Hadar M. 2000. *Migrating soaring birds align along sea-breeze fronts; First evidence from Israe*l. Bull. Am. Meteorol. Soc. 81, 7: 1599-1601.

Atlas D. 1964. *Advances in Radar Meteorology.* Adv. Geophys. 10: 318-468.

Bahat O., Ovadia O. 2005. *Minimizing Bird-Aircraft Collisons Caused by Resident Raptors in Israel.* IBSC 27th Meeting, Athens, Hellas, 23-27 May 2005: p. 178.

Bruderer B., Joss J. 1969. *Zur Registrierung and Interpretation von Echosingnaturen an enema 35 cm-Zielvervolgungstradar.* Orn. Beob. 66: 70-88.

Bruderer B. 1992. *Radar studies on Bird migration in the south of Israel.* BSCE/21, Jerusalem: pp. 269-280.

Bruderer B., Liechti F. 1995. *Variation in density and height distribution of nocturnal migration in the south of Israel*. Isr. J. Zool. 41, 3: 477-489.

Bruderer B. 1997. *Migratory directions of birds under the influence of wind and topography.* RIN Symposium Orientation & Navigation – Birds, Humans & other animals. Oxford. 27/1-10.

Buurma L. 1999. *The Royal Netherlands Air Force: Two Decades Of Bird Strike Prevention "En Route"*. International Seminar on Birds and Flight Safety in the Middle East, Israel, April, 25-26, 1999: pp. 71-83.

Chernikov A., 1979. [*Radar clear sky echoes*.] Hydrometeoizdat, Leningrad: 3-40. (In Russian).

Chernikov A., Schupjatsky A. 1967. [*Polarization characteristics of radar clear sky echoes*.] Transactions of USSR academy of sciences, atmosphere and ocean physics 3, 2: 136-143. (In Russian).

Dinevich L., Kapitalchuk I., Schupjatsky A. 1994. [*Use of the polarization selection of radar signals for remote sounding of clouds and precipitation*.] 34th Israel Annual Conference on Aerospace Science: pp. 273-277.

Dinevich L., Leshem I., Gal A., Garanin V., Kapitannikov A. 2000. *Study of birds migration by means of the MRL-5 radar.* Sci. Isr. – Technol. Adv. 4.

Dinevich L., Leshem Y., Pinsky M., Sterkin A. 2004. D*etecting birds and estimating their velocity vectors by means of MRL-5 meteorological radar.* Ring 26, 2: 35-53.

Eastwood E. 1967. *Radar ornithology.* Methuen, London: 278.

Edwards J., Houghton E.W. 1959. *Radar echoing area polar. Diagrams of birds*. Nature 184, 4692.

Doviak R., Zrnic D. 1984. *Doppler Radar and Weather Observation*. Acad. Press: 512 pp.

Ganja I., Zubkov M., Kotjazi M. 1991. [*Radar ornithology.*] Stiinza, pp. 123-145. (In Russian).

Gauthreaux S.A., Belser C.G. 2003. R*adar ornithology and biological conservation*. Auk 120, 2: 266-277.

Gauthreaux S.A., Sidney A.Jr., Mizrahi D.S., Belser C.G. 1998. *Bird Migration and Bias of WSR–88D Wind Estimates.* Weather and Forecasting 13: 465-481.

Glover K., Hardy K. 1966. *Dot angels: insects and birds*. Proc. 12th Weather Radar Conf., Amer. Met. Soc., Boston, 1966: pp. 264-268.

Gudmundsson G.A., Alerstam T., Green M., Hedenström A. 2002. *Radar observations of Arctic bird migration at the Northwest Passage, Canada*. Arctic 55, 1: 21-43.

Hajovsky R., Deam A., La Grone A. 1966. *Radar reflections from insects in the lower atmosphere*. IEEE Trans. on Antennas and Propagation 14: 224-227.

Hardy K.R., Katz I. 1969. *Probing the Atmosphere with High Power, High Resolution Radars*. Panel on Remote Atmospheric Probing of the National Academy of Sciences, Chicago, Ill.

Houghton E 1964. *Detection, recognition and identification of birds on radar.* World conf. Radio Met., Amer. Met. Soc., Boston: pp. 14-21.

Komenda-Zehnder S., Liechti F., Bruderer B. 2002. *Is reverse migration a common feature of nocturnal bird migration. An analysis of radar data from Israe*l. Ardea 90, 2: 325-334.

Kropfli R.A. 1970. *Simultaneous radar and instrumented aircraft observations in a clear air turbulent layer.* Prepr. 14th Radar Met. Conf., Amer. Met. Soc., Boston: pp. 117-120.

Larkin R.P., Evans W.R., Diehl R.H. 2002. *Nocturnal flight calls of Dickcissels and Doppler radar echoes over south Texas in spring*. J. Field Ornithol. 73, 1: 2-8.

Leshem Y., Gauthreaux S.A. 1996. *Proposal to develop a global network to predict bird movements on a real-time and daily scale by using radars. Bird Strike Committee Europe BSCE-23/WP 50*. London, May 13-17, 1996.

Leshem Y., Yom-Tov Y. 1996. *The use of thermals by soaring migrants in Israel*. Ibis 138: 667-674.

Leshem Y., Yom-Tov. Y. 1998. *Routes of migrating soaring birds*. Ibis 140: 41-52.

Lofgren G., Battan L. 1969. *Polarization and vertical velocities of dot angel echoes*. J. Appl. Met. 1969: 948-951.

Miller M.A., Verlinde J., Gilbert C.V., Lehenbauer G.J., Tongue J.S., Clothiaux E.E. 1998. D*etection of nonprecipitating clouds with the WSR-88D: a theoretical and experimental survey of capabilities and limitations.* Weather and Forecasting 13, 4: 1046-1062.

Richardson W.J., West T. 2005. *Serious Birdstrike Accidents to U. K. Military Aircraft, 1923 to 2004: Numbers and Circumstances*. IBSC 27th Meeting, Athens, Hellas, 23-27 May 2005: p. 5.

Russell K.R., Gauthreaux S.A. 1998. *Use of weather radar to characterize movements of roosting purple martins*. Wildl. Soc. Bull. 26, 1: 5-16.

Schupjatsky A. 1959. [*Radar dispersion by non-spherical particles*.] CAO Tr. 30: 39-52. (In Russian).

Skolnik M. 1970. *Radar handbook.* McGraw-Hill Book Company.

Stepanenko V. 1973. [*Radar in meteorology.*] Hydrometeoizdat, Leningrad. (In Russian).

Thorpe J. 2005. *Fatalities and Destroyed Civil Aircraft Due to Bird Strikes, 2002 to 2004 (with an Addendum of Animal Strikes)*. IBSC 27th Meeting, Athens, Hellas, 23-27 May 2005: pp. 17-24.

Venema V., Russchenberg H. 2000. *Clear-air scattering observations: downdraft and angels*. Physics and Chemistry of the Earth. B: Hydrology 25, 10-12: 1123-1128.

Zavirucha V., Saricev V., Stepanenko V, Shepkin U., 1977. [*Study of the dispersion characteristics of the meteorological and ornitological objects in echo-free cameras.*] Proc. Main Geophysic Observatory 395: 40-45. (In Russian).

Zrnic D.S., Ryzhkov A.V. 1998. *Observations of insects and birds with a polarimetric radar.* IEEE Transactions on Geoscience and Remote Sensing 36, 2: 661-668.